Design of Semi-Submersible Platform using Computational Fluid Dynamics

K. Rohit Kumar, M. Ravishankar, R. Harish

Abstract: ***This paper reports based on an experimental study to simulate flow due to irregular fluid flow in a semi-submersible platform using computational fluid dynamics. In this paper we use computational fluid dynamics tools which solve simple differential equations and finite volume method (FVM). A turbulence model is considered i.e. large eddy simulation (LES). The semi-submersible model is considered as pontoons, columns, horizontal brace and deck. The pontoons are horizontal placed stadium shaped structures which are submerged into the water. The columns are structures which connect the deck and pontoons in these model circular columns are considered. The horizontal braces are circular tube-like structures which connect the two or more columns which increases the rigidity of the columns. The deck is a flat surface which provides workable area. This paper is a comparison of fluid flow at different velocity magnitude. The velocity contour, pressure contour and streamline contour are simulated and graphically represented. The numerical simulations are compared with experimental solutions and focus on vicinity of the platform. The difference in pressure, temperature and streamline flow are tabulated and graphically represented. The average percentage difference in temperature and pressure are calculated to be 73% and 128% respectively. Thus, the causation is investigated for the case and several governing parameters are recognized.***

Keywords: ***Semi-submersible, Computational fluid dynamics (CFD), Finite volume method (FVM), Large eddy simulation (LES), circular column.***

I. INTRODUCTION

A semi-submersible platform is a specialized marine vessel used which is used for offshore roles such as oil mines, drilling rigs, safety vessels and also for heavy lift cranes. These platforms were designed and developed for oil mines in early 1960s. These semi-submersible platforms are employed in offshore drilling in high water depths i.e. greater than 520 meters where fixed structures are not practical possible. The semi-submersible has good stability which is far better than drill ships. There are many possible failures and disasters that accompany these structures such as lift and drag forces in particular. This paper is an experimental study due to an incoming regular wave in a semi-submersible platform using computational fluid dynamics.

Revised Manuscript Received on February 28, 2020.
*Correspondence Author
K. Rohit Kumar, Postgraduate Student, M.Tech CAD/CAM, School of Mechanical Engineering, Vellore Institute of Technology Chennai, Tamilnadu, India.
M. Ravishakar, Postgraduate Student, M.Tech CAD/CAM, School of Mechanical Engineering, Vellore Institute of Technology Chennai, Tamilnadu, India.
R. Harish*, Assistant Professor, Thermal and Automotive Research Group, School of Mechanical Engineering, Vellore Institute of Technology Chennai, Tamilnadu, India. E-mail: harish.r@vit.ac.in

Qiu et al, [1] performed experiments in optimization of semi-submersible platforms and found the prediction of the motion response by using the computational fluid dynamics tool. They measured the hydrodynamic performances during optimization process and the total weights can be reduced. Travanca et al, [2] performed experiments in a control of vibrations induced wave on floating production systems and found the large environmental force acts on offshore structures. They measured the motion of offshore production units with the dynamics and vibration control of floating structures due to wave loading and analysis the performance model by using computational fluid dynamics. Jin et al, [3] performed experiments in a wave simulations and fluctuating wind on a semi-submersible offshore platform and they observed the wind and wave simulations in structural analyses. They monitor the health of several offshore platforms. Raed et al, [4] performed experiments in extreme hydrodynamic responses of semi-submersible platforms and they observed the two different environmental contour approaches. Adopting different environmental contour approaches has small deviation between the significant wave heights. Liang et al, [5] performed experiments in vortex-induced motions of a deep-draft semi-submersible platform and found the VIM effects on the overall hydrodynamics of the structure. They measured the lift and drag forces on the structure in horizontal plane transverse motion. Xing et al, [6] performed experiments in a semi-submersible crane vessel to optimize the quantity, locations and output current of anode to improve cathodic protection and they observed the numerical simulation result for the semi-submersible crane vessel and also predict the cathodic protection effect for four different stages. Wei et al, [7] performed experiments in an effect of bracings and motion coupling on semi-submersible platform under irregular wave conditions and they validate the wave basin test and numerical simulations. They also observed the motion results in semi-submersible platform. Liu et al, [8] performed experiments in a design loads for a large wind turbine in a semi-submersible floating platform and they observed the dynamic response and reliability analysis of a offshore wind turbine and appropriate response quantile level has produced by using the inverse first-order reliability method.

The objective of the present study is to investigate the turbulent flow around a semi-submersible platform. The semi-submersible model is placed inside a channel and fluid flow is simulated as large eddy simulation model. The boundary conditions at the inlet are velocity-inlet and the outlet boundary condition is pressure-outlet. The velocity magnitude is varied along the x-direction as 5m/s and 10m/s.

The numerical simulations are performed by using a Finite Volume Method (FVM). The fluid medium used in this model is air. The resulted values for pressure and velocity are recorded at specific locations and tabulated for different velocity magnitudes. The percentage difference between pressure and velocity for both cases are tabulated. The average percentage difference is calculated. The various contour of velocity, pressure and the streamline flow are represented in figures. Thus, several governing parameters are investigated and the flow characteristics are analyzed.

II. GOVERNING EQUATIONS AND NUMERICAL TECHNIQUE

The basic parts of a semi-submersible are pontoons, columns, horizontal brace and deck as shown in the figure 1. The pontoons are horizontal structures which placed at the bottom of the semi-submersible platform and are totally submerged into the waters. The columns are structures which withstand the weight of the semi-submersible platform and also connect the deck and pontoons. The horizontal braces are structures which connects the two or more columns. The deck are surfaces upon which all the humans, machinery and other equipment's are placed.

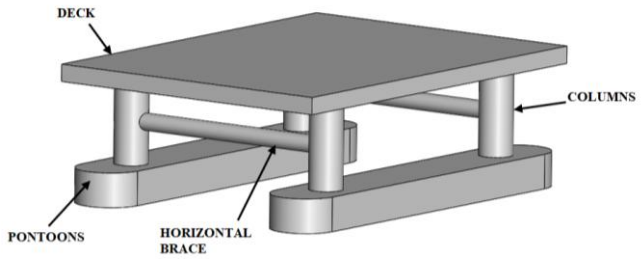

Figure 1. 3D representation of semi-submersible

The semi-submersible is modelled with dimensions of length 'L_1' = 120m and total height 'H' = 40m as shown in figure 2. The diameter of the column is denoted as L_c = 10m and height of the column is denoted as H_c = 25m as shown in figure 2. The length 'L_2' = 90m and the length of pontoons is equal to the length L_1. The height of the pontoon Hp = 10m as shown in figure 3. The length of the horizontal brace L_b = 60m and diameter of the column H_b = 5m as shown in the figure 3. The model is created using solid works and imported into designer modeler in ANSYS workbench. The fine meshing was done using fluent.

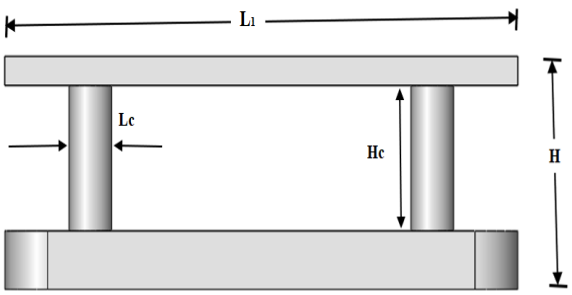

Figure 2. 2D representation of semi-submersible

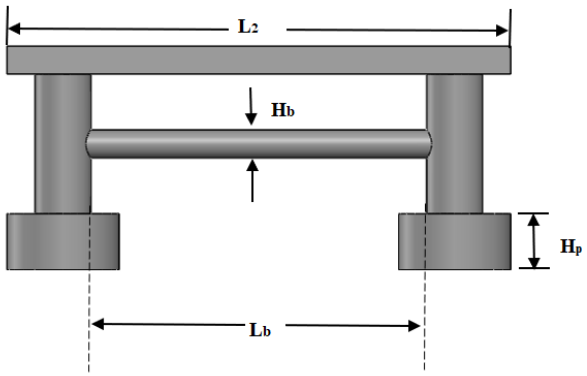

Figure 3. 2D representation of semi-submersible

The model considered in the present study is of 120 m long, 90 m wide and 40 m high semi-submersible. The model is centrally placed inside a channel through which fluid is simulated along the x-direction. The type of solver used pressure-based and absolute velocity formulation is used. A turbulence model is used and large eddy simulation LES and smagorinsky-lilly sub grid-scale model is considered. The boundary conditions along x -axis at the inlet is Velocity-inlet and the outlet boundary condition is pressure-outlet and no slip boundary condition are considered along the walls. The residual for continuity, x-velocity, y-velocity and z-velocity is considered to be 0.001. The velocity magnitude in the x-direction is compared between 5m/s and 10m/s. The numerical simulations are performed by using a Finite Volume Solver (FVM), where the problem is modeled as buoyancy induced turbulent flows. The turbulent flow problem is modeled by solving the large eddy simulation (LES) equation for different velocity [9-14]. The time averaged governing equations are as follows:

$$\frac{\partial \overline{u_i}}{\partial t} + \frac{\partial \overline{u_i}}{\partial x_i} = 0 \quad (1)$$

$$\frac{\partial \overline{u_i}}{\partial t} + \overline{u_j}\frac{\partial \overline{u_i}}{\partial x_j} = -\frac{1}{\rho}\frac{\partial \overline{p}}{\partial \overline{x_i}} + \frac{\partial}{\partial x_j}\left[\upsilon \frac{\partial \overline{u_i}}{\partial x_j} - \overline{u_i' u_j'}\right] \quad (2)$$

$$\frac{\partial \overline{T}}{\partial t} + \overline{u_i}\frac{\partial \overline{T}}{\partial x_i} = \frac{\partial}{\partial x_i}\left[\alpha \frac{\partial \overline{T}}{\partial x_i} - \overline{u_i' T'}\right] \quad (3)$$

$$\frac{\partial k}{\partial t} + \overline{u_i}\frac{\partial k}{\partial x_i} = \frac{\partial}{\partial x_i}\left[\frac{\upsilon_t}{\sigma_k}\frac{\partial k}{\partial x_i}\right] + \upsilon_t\left[\frac{\partial \overline{u_i}}{\partial x_j} + \frac{\partial \overline{u_j}}{\partial x_i}\right]\frac{\partial \overline{u_i}}{\partial x_j} - \varepsilon \quad (4)$$

$$\frac{\partial \varepsilon}{\partial t} + \overline{u_i}\frac{\partial \varepsilon}{\partial x_i} = \frac{\partial}{\partial x_i}\left[\frac{\upsilon_t}{\sigma_k}\frac{\partial \varepsilon}{\partial x_i}\right] + C_{1\varepsilon}\frac{\varepsilon}{k}\upsilon_t\left[\frac{\partial \overline{u_i}}{\partial x_j} + \frac{\partial \overline{u_j}}{\partial x_i}\right]\frac{\partial \overline{u_i}}{\partial x_j} - C_{2\varepsilon}\frac{\varepsilon^2}{k} \quad (5)$$

Where ‘ρ’ indicates the density of fluid, ‘u’ represents the velocity, ‘k’ and ‘ε’ indicates the kinetic energy and dissipation fields.

III. RESULTS AND DISCUSSION

Figure 4 indicates the pressure contour for velocity magnitude of 5 m/s in the present study. The air is supplied through the inlet along the x-direction in a channel. Due to the air pressure in the channel moving along the x-direction, the flow is converged at vicinity near the columns where pressure at low identified along the y-direction as shown in the figure 4. The figure 5 represents the velocity contour for velocity magnitude of 5 m/s. A high velocity is identified at the behind each column when fluid is passed along the inlet in the x-direction and significant low velocity at the vicinity of the columns. In the figure 6 the streamline velocity is represented in which it shows the direction of fluid flow. A turbulent effect is seen at the columns and horizontal brace. In the vicinity near the column low velocity streamline are reported and slight increase in velocity is noted behind the column. Similar to the previous study and velocity magnitude is increased to 10m/s. When the fluid is channel through the inlet in the x-direction the pressure, velocity & streamline results are concluded. In the figure 7 the pressure contour is 10 m/s are resulted which is compared to the previous obtained results of 5m/s. The results are compared the found to be increased significantly along the x-direction. The low-pressure region is found above the horizontal brace similar results were found in 5m/s. In the figure 8 represents the velocity contours, there is increase in velocity value. In the figure 9 the streamline velocity is represented which shows the turbulence near the semi-submersible.

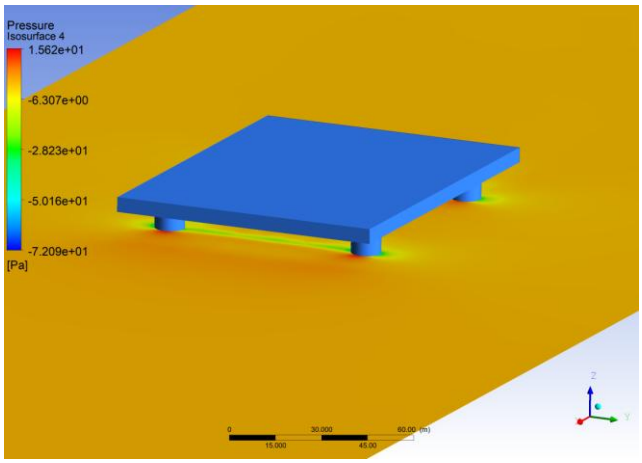

Figure 4. Pressure contours for velocity 5 m/s

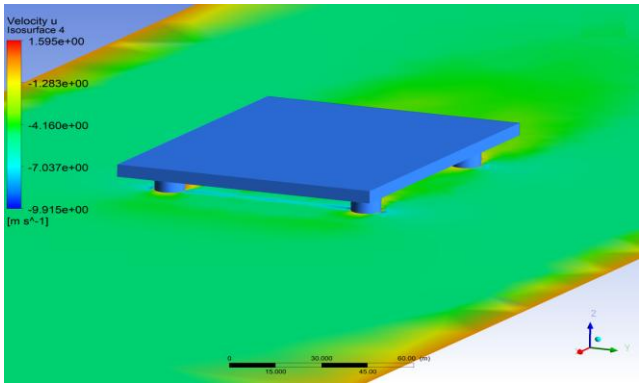

Figure 5. Velocity contours for velocity 5 m/s

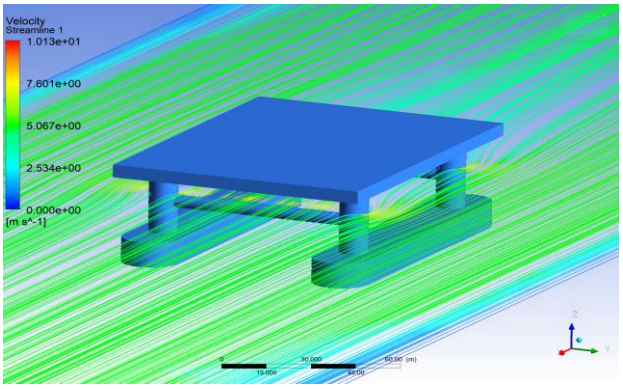

Figure 6. Streamline velocity for velocity 5 m/s

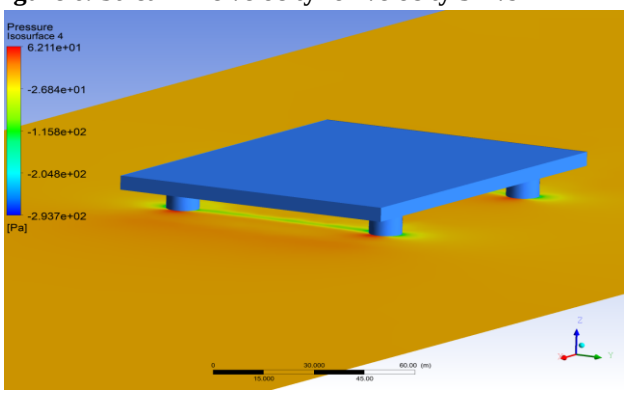

Figure 7. Pressure contours for velocity 10 m/s

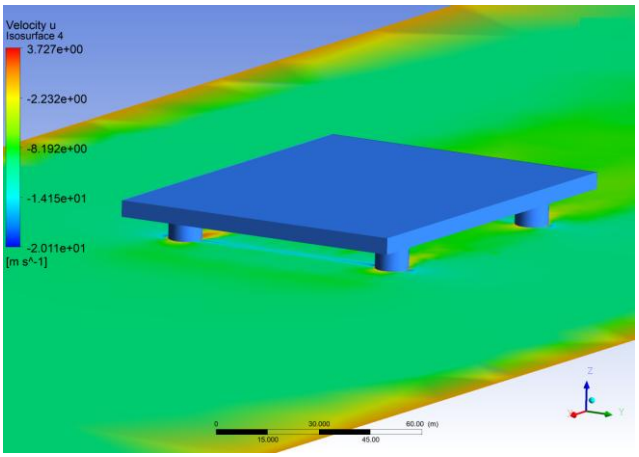

Figure 8. Velocity contours for velocity 10 m/s

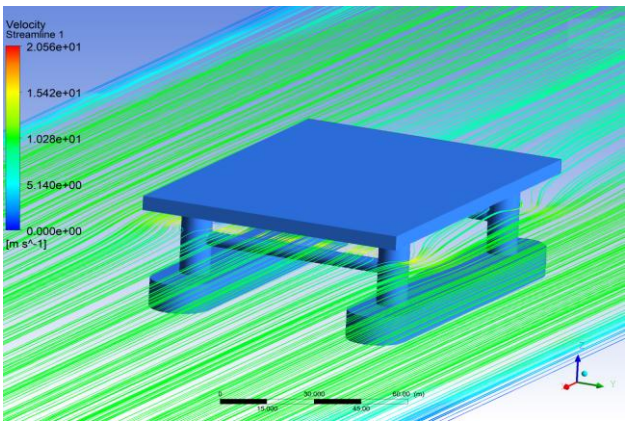

Figure 9. Streamline velocity for velocity 10 m/s

Table 1 Variation of pressure and velocity

X-Axis	5 m/s		10 m/s	
	Pressure (Pa)	Velocity (ms^{-1})	Pressure (Pa)	Velocity (ms^{-1})
10	-5.674	0.330	-22.259	0.397
0	-4.661	0.075	-18.110	1.432
-10	6.736	-3.081	0.616	-5.253
-20	0.333	-3.747	1.346	-7.264
-30	0.471	-3.989	1.921	-8.013
-40	0.768	-4.189	3.404	-8.358
-50	2.237	-4.197	9.936	-8.334
-60	11.950	-1.089	50.279	-2.230

The figure 10 is a graphically representation of velocity difference between 5m/s and 10m/s. The coordinate's x-axis is varied from 10 to -60 where the y-axis and z-axis are kept constant as 35 and 20 respectively. The values are noted at several intervals which are tabulated in table 1. Note-the values are considered between the columns. The velocity tends to increase at vicinity column and then decreases significantly later. The figure 11 is a graphically representation of pressure difference at 5 m/s and 10 m/s. Similar co-ordinates are considered which was taken in the velocity difference. Equal interval of 10 m is taken and the results are noted as shown in table 1. The pressure behind the column is comparatively less and further increases along the x-direction. The red & square symbolled line represents the velocity at 5 m/s and blue & circle symbolled line represents the velocity at 10 m/s.

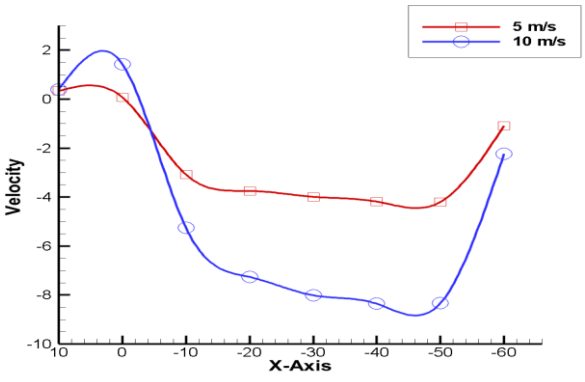

Figure 10. Graphically representation of velocity difference

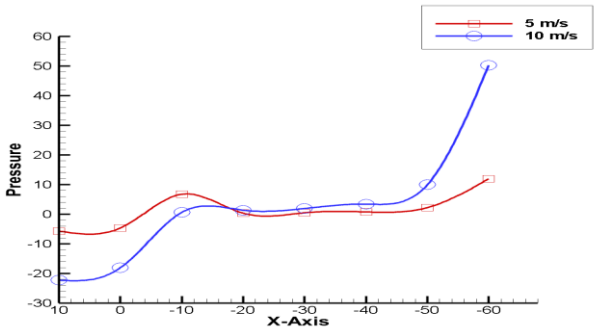

Figure 11. Graphically representation of pressure difference

Table 2 Difference in pressure & velocity in x-axis

X-Axis	Difference in pressure (%) (Pa)	Difference in velocity (%) (ms^{-1})
10	118.75	18.43
0	118.13	180.11
-10	166.47	52.13
-20	120.74	63.88
-30	121.29	67.05
-40	126.33	66.46
-50	126.50	66.03
-60	123.20	68.77
Average	127.68	72.86

The table 2 represents the percentage difference between the pressure of 5m/s and 10m/s similarly for velocity difference between the velocities of 5m/s and 10m/s. The percentage difference is calculated by taking the difference between the values and dividing average between the considered values and then multiplied by 100. Therefore, the results are obtained for pressure and velocity as shown in table 2.

IV. CONCLUSION

The fluid flow characteristics across a semi-submersible through a channel are numerically investigated by varying the velocity magnitude. The turbulent flow is modeled by the computational fluid dynamics (CFD) approach using and large eddy simulation (LES) Smagorinsky-Lilly model and the governing equations are discretized using finite volume method (FVM). The stream line patterns, velocity and pressure contours are analyzed for different velocity magnitude. A comparison is made between varied velocity magnitude and it is found the characteristics in pressure and velocity. The stream line contours indicated the flow direction of the fluid of a semi-submersible through a channel. It is identified that the velocity decreases between the columns and higher difference are found when velocity magnitude increases. The pressure difference slightly reduces at the vicinity of the column and tends to increase further. The pressure near the second column is significantly higher when velocity magnitude increases. In further research by introducing a pencil column may reduce the pressure values in the second column which may reduce the stress in the structure. The results from the present study will be suitable for designing semi-submersible platforms which are used in oil productions and deep seas applications.

EFERENCES

1. W. Qiu, X. Song, K. Shia, X. Zhang, Z. Yuan, Y. You, Multi-objective optimization of semi-submersible platforms using particle swam optimization algorithm based on surrogate model. Ocean Engineering 178(2019), pp 388-409.
2. J. Travanca, H. Hao, Control of wave-induced vibrations on floating production systems, Ocean Engineering 141(2017), pp 35-52.
3. J. Ma, D. Zhou, Z. Han, K. Zhang, Y. Bao, L. Dong, Fluctuating wind and wave simulations and its application in structural analysis of a semi-submersible offshore platform, International Journal of Naval Architecture and Ocean Engineering 11(2019), pp 624-637.

4. K. Raed, A.P. Teixeira, C. G. Soares, Uncertainty assessment for the extreme hydrodynamic responses of a wind turbine semi-submersible platform using different environmental contour approaches, Ocean Engineering.
5. Y. Liang, L. Tao, L. Xiao, M. Liu, Experimental and numerical study on vortex-induced motions of a deep-draft semi-submersible, Applied Ocean Research Volume 67, September 2017, pp 169-187.
6. S.H. Xing, Y. Li, H.Q. Song, Y.G. Yan, M.X. Sun, Optimization the quantity, locations and output currents of anodes to improve cathodic protection effect of semi-submersible crane vessel, Ocean Engineering 113(2016), pp 144- 150.
7. H. Wei, L. Xiao, Y. M. Low, X. Tian, M. Liu, Effects of bracings and motion coupling on resonance features of semi-submersible platform under irregular wave conditions, Journal of Fluids and Structures 92(2020), pp 102783.
8. J. Liu, E. Thomas, A. Goyal, L. Manuel, Design loads for a large wind turbine supported by a semi-submersible floating platform, Renewable Energy 138(2019), pp 923-936.
9. R.Harish, Buoyancy driven turbulent plume induced by protruding heat source in vented enclosure, International Journal of Mechanical Sciences,2018,pp:209-222.
10. R.Harish, Effect of heat source aspect ratio on turbulent thermal stratification in a naturally ventilated enclosure, Building and Environment, 2018,pp:473-486.
11. R.Harish, K.Venkatasubbaiah, Non-Boussinesq approach for turbulent buoyant flows in enclosure with horizontal vent and forced inlet port, Applied Mathematical Modelling, 2016,pp:927-941.
12. R.Harish, K.Venkatasubbaiah, Numerical investigation of instability patterns and nonlinear buoyant exchange flow between enclosures by variable density approach, Computers & Fluids, 2014,pp:276-287.
13. R.Harish, K.Venkatasubbaiah, Mathematical modeling and computation of fire induced turbulent flow in partial enclosures, Applied Mathematical Modelling,2013,pp:9732-9746.
14. R.Harish, K.Venkatasubbaiah,Numerical simulation of turbulent plume spread in ceiling vented enclosure, European Journal of Mechanics-B/Fluids,2013,pp:142-158.

AUTHORS PROFILE

K. Rohit Kumar, is pursuing his M.Tech degree in CAD/CAM at VIT Chennai campus and has completed B.Tech mechanical in SRM university. His field of interests are CFD and CAD.

M. Ravishakar, is pursuing M.Tech degree in CAD/CAM at VIT Chennai campus and has completed B.Tech mechanical in M Kumarasamy College. His research interests are in the field of CFD & Heat Transfer.

Dr. R. Harish, is working as an Assistant Professor in the school of Mechanical Engineering at VIT Chennai campus. His research interests are in the field of computational fluid dynamics, Heat Transfer and Turbulent flows.